SAND2015-4213C

Exceptional service in the national interest

Sandia National Laboratories

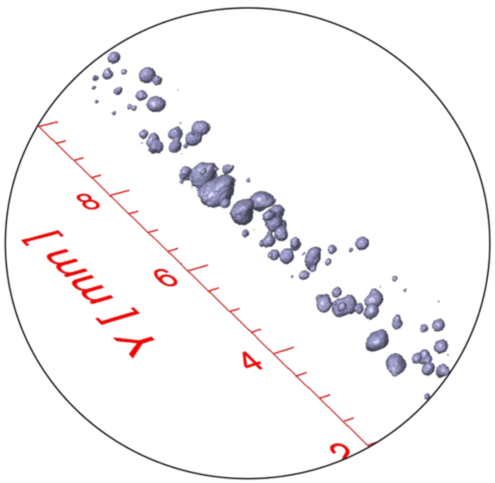

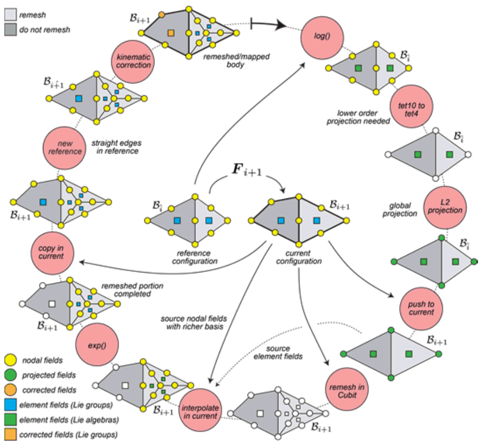

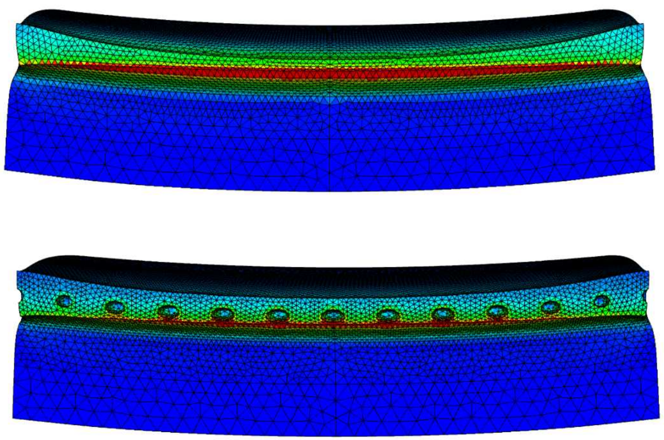

Resolving the evolution of pore structures in 304-L laser welds

J. Foulk, M. Veilleux, J. Emery, J. Madison, H. Jin, J. Ostien, A. Mota

3rd TMS ICME, Colorado Springs, June 2015

U.S. DEPARTMENT OF ENERGY

NNSA National Nuclear Security Administration

Sandia National Laboratories is a multi-program laboratory managed and operated by Sandia Corporation, a wholly owned subsidiary of Lockheed Martin Corporation, for the U.S. Department of Energy's National Nuclear Security Administration under contract DE-AC04-94AL85000. SAND NO. 2011-XXXXP

Failure is the loss of load-bearing capacity

Austenitic stainless steels are extremely tough and damage tolerant

The failure of 304-L is a necking problem. Free surface creation is a 2nd order effect.

Hypothesis: Pore size and distribution can aid the necking process

- μ-CT needed to probe initial and interrupted pore structures
- Remeshing/mapping needed to resolve the evolution of pore structure
- Homogenization not applicable

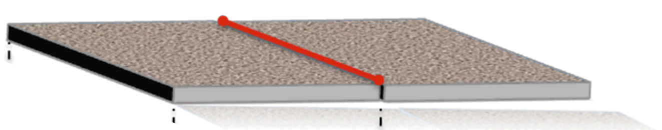

304-L butt weld

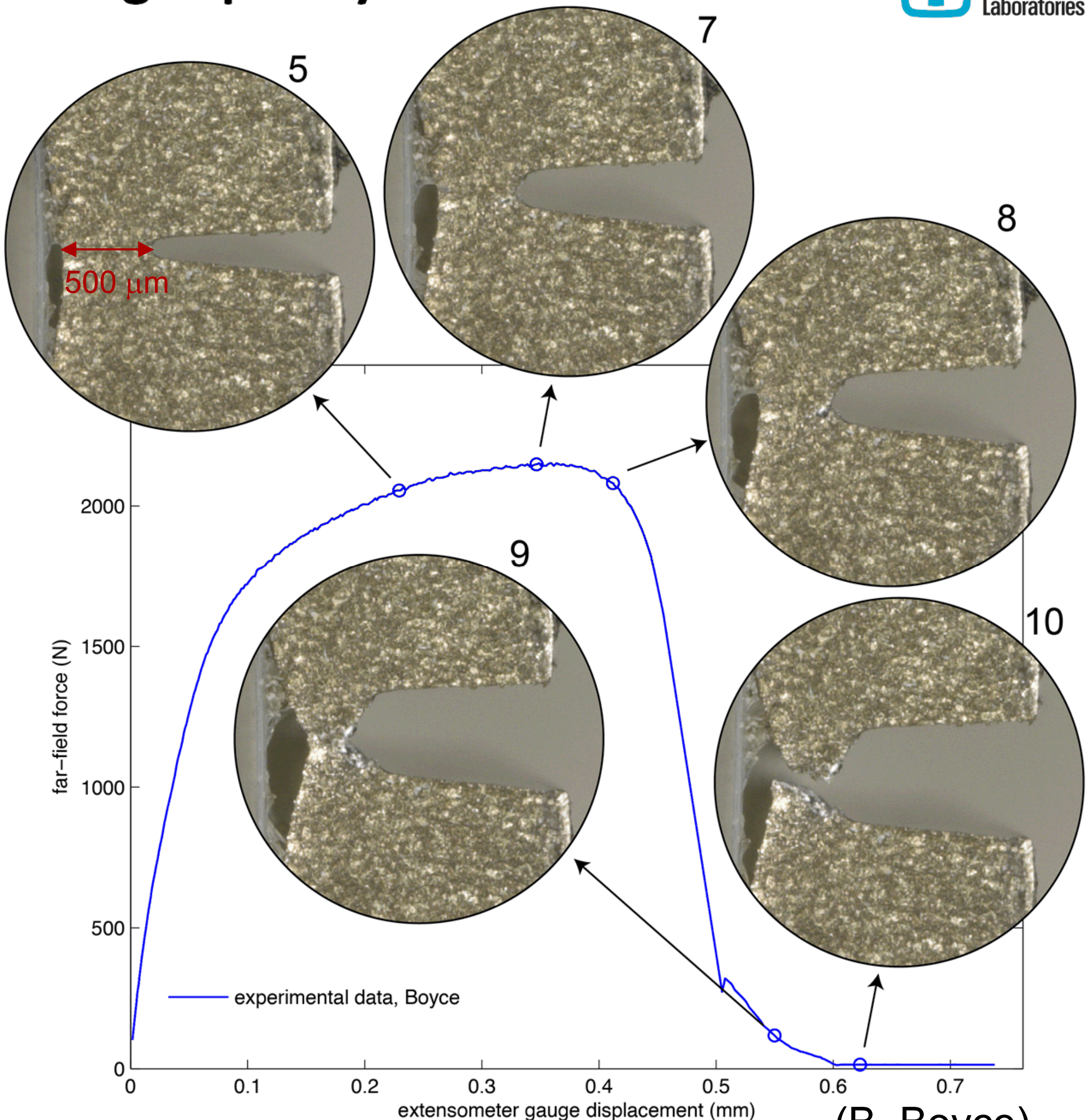

(B. Boyce)

Pores large relative to the ligament – homogenization n/a

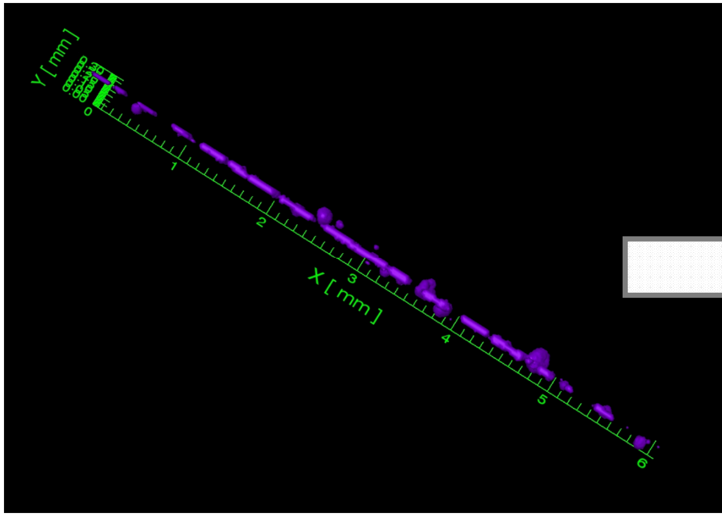

μ-Computed Tomography

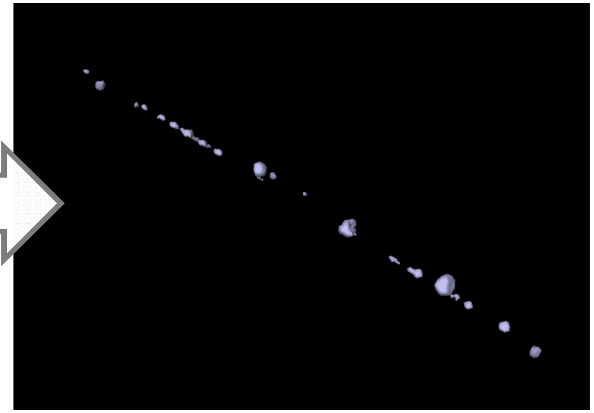

Magnification: 9X
Voxel size: 14 μm
Energy: 130 keV

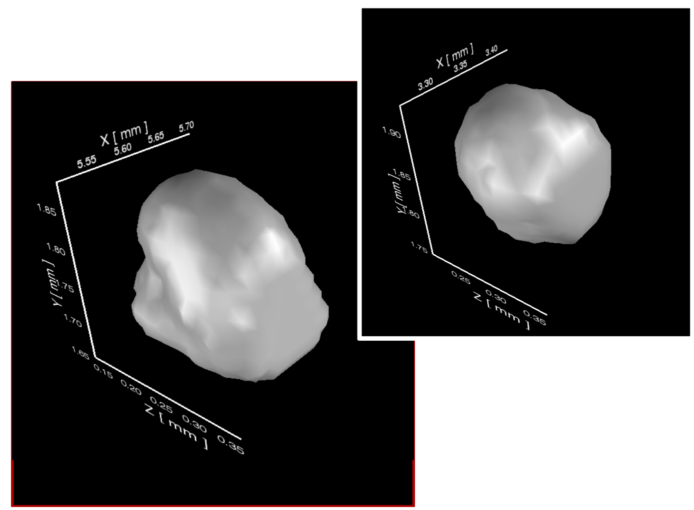

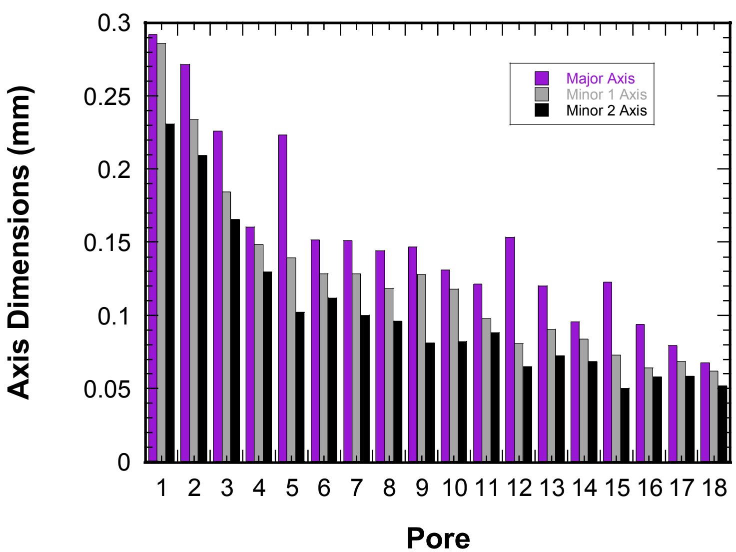

J. Madison, L. K. Aagesen, *"Quantitative Characterization of Porosity in Laser Welds of Stainless Steel"* SCRIPTA MATERIALIA (2012)

Do the pores dominant the deformation process?

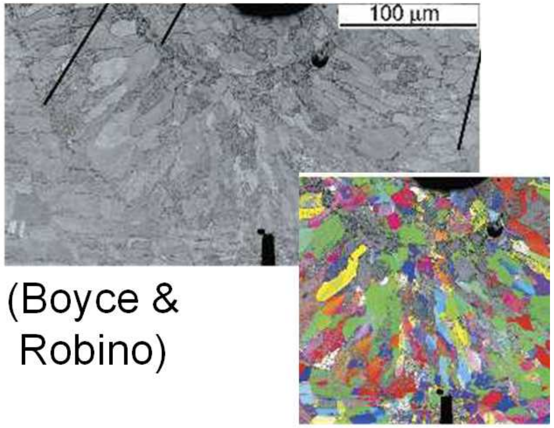

(Boyce & Robino)

What elements of microstructure dominate the load-bearing capacity?

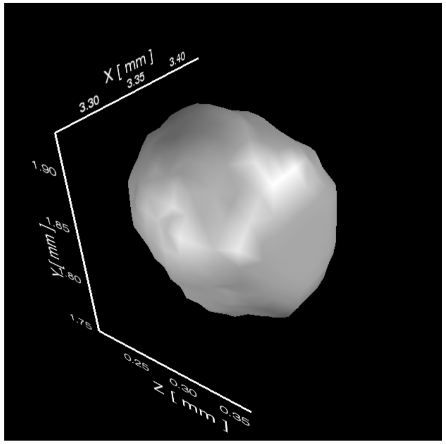

(Madison)

- We hypothesize that pores are the dominant microstructural feature
- We adopt J_2 plasticity for both the base material and the weld
- We have lumped dislocation structures, deformation twinning, and martensitic phase transformations into a phenomenological model for hardening and recovery

sheet thickness: 1.6 mm
ligament length: 508 µm
pore diameter: 150 µm
area fraction: 0.066

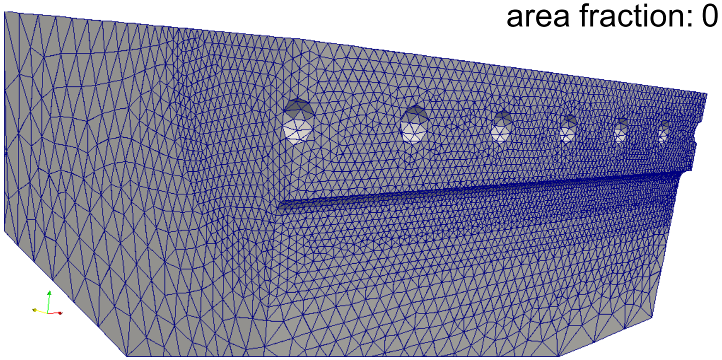

NOTE: Unlike experiments, simulation can systematically increase complexity. Pores first.

Initial efforts w/pores problematic – remeshing needed

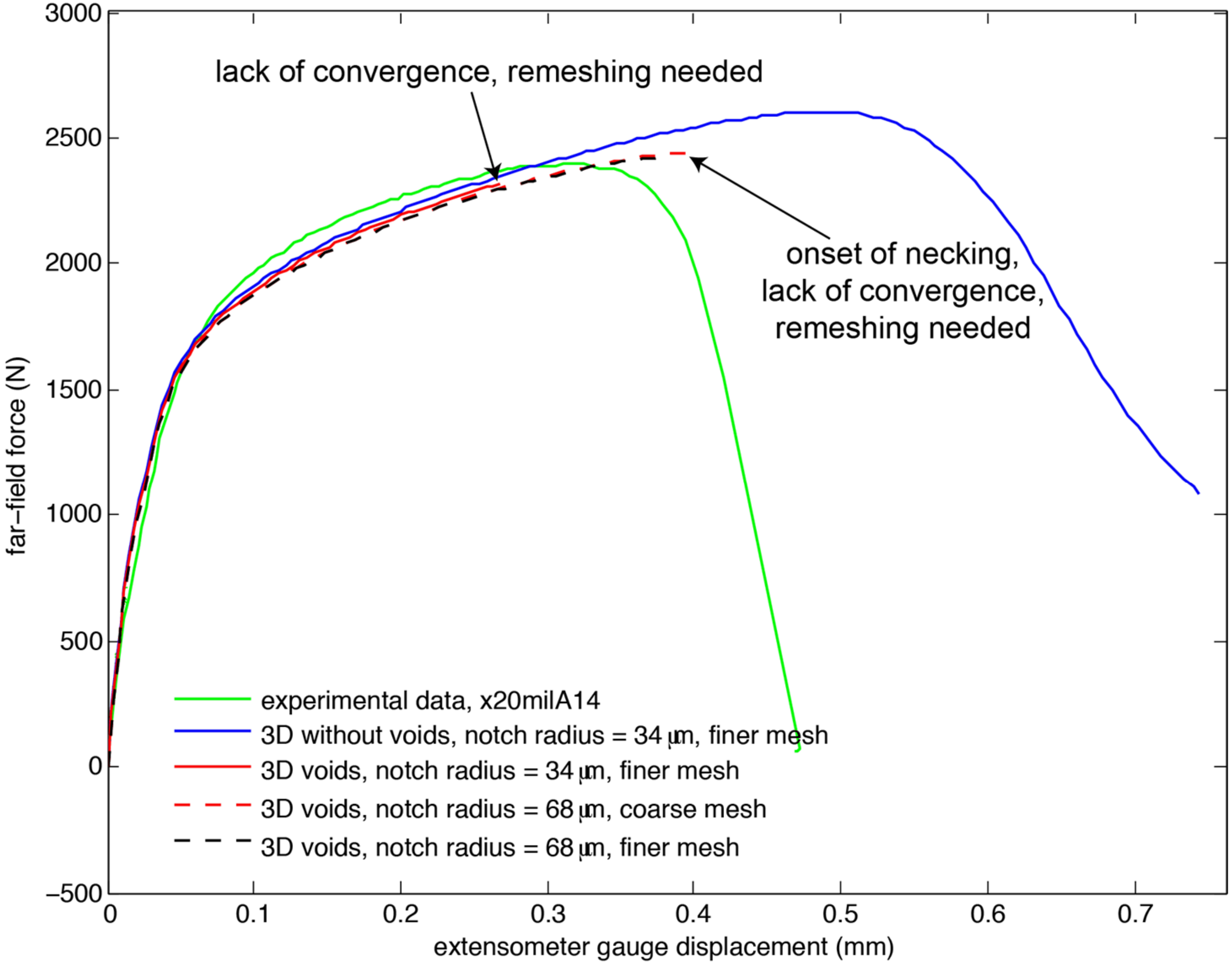

notch radius: 68 μm

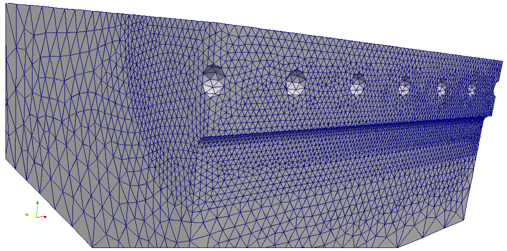

Onset of necking
notch radius = 68 μm
coarse mesh

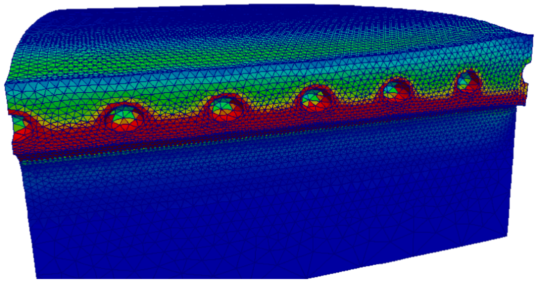

NOTE: Same constitutive model employed for cases with and without voids

Deeper-penetration welds provide additional motivation

Weld schedule impacts porosity. Porosity impacts performance.

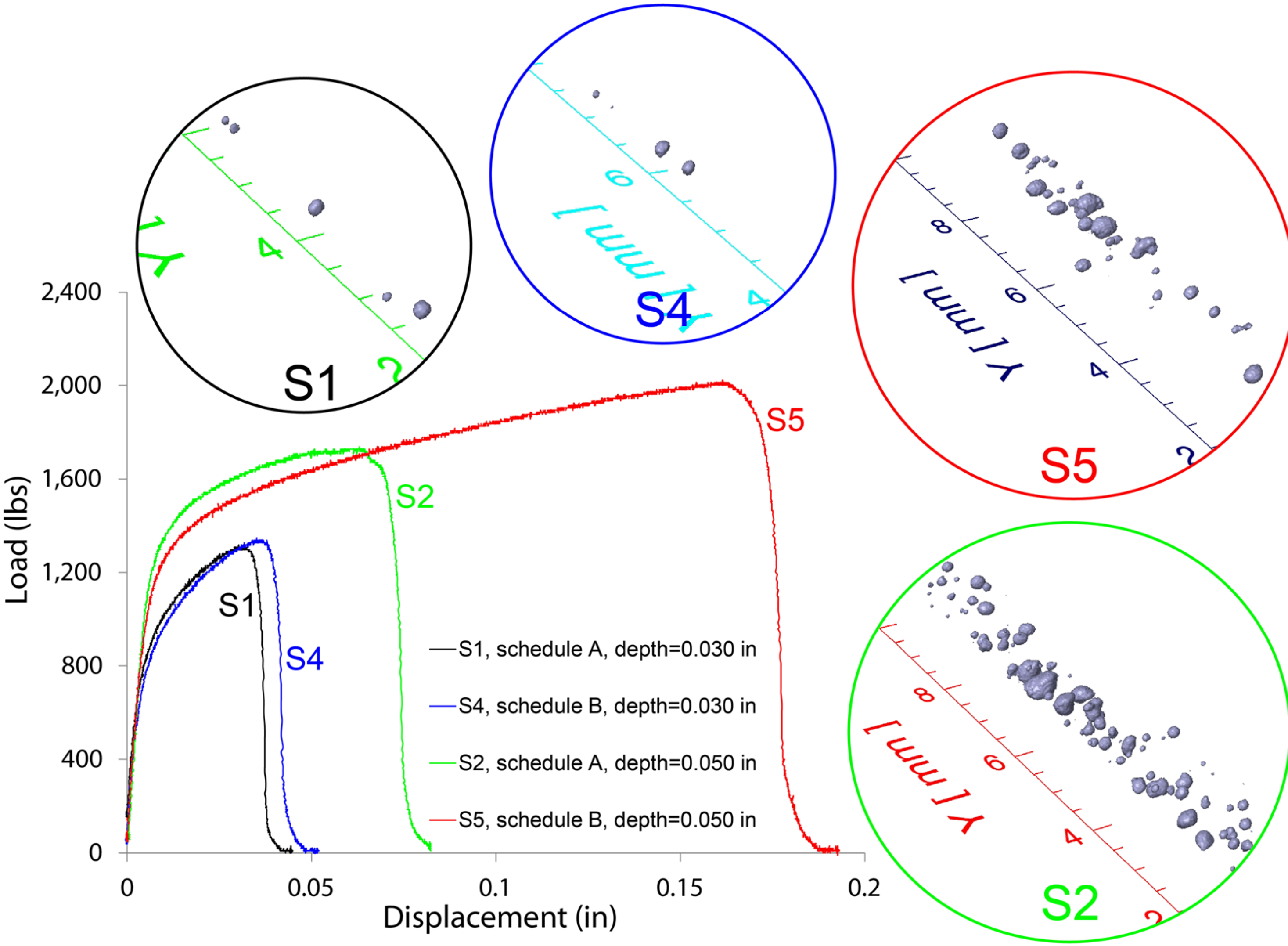

Given the void structure (shape, size, location), can we predict these findings?

(H. Jin, J. Madison)

Our approach: mapLL (L_2 + Lie Group/Algebra)

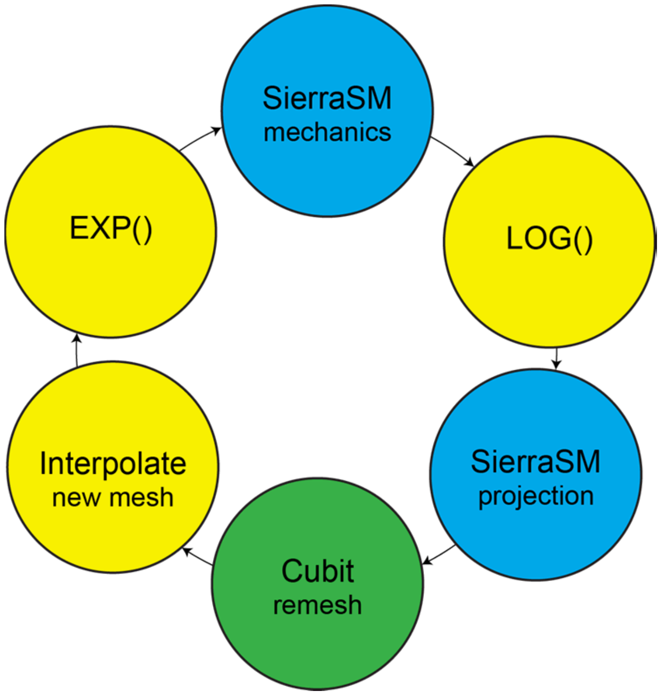

$$\Phi[\boldsymbol{\varphi}, \bar{\boldsymbol{z}}, \bar{\boldsymbol{y}}] := \int_B W(\boldsymbol{F}, \bar{\boldsymbol{z}})\, dV + \int_B \bar{\boldsymbol{y}} \cdot (\bar{\boldsymbol{z}} - \boldsymbol{z})\, dV - \int_B \rho_0 \boldsymbol{B} \cdot \boldsymbol{\varphi}\, dV - \int_{\partial_T B} \boldsymbol{T} \cdot \boldsymbol{\varphi}\, dS$$

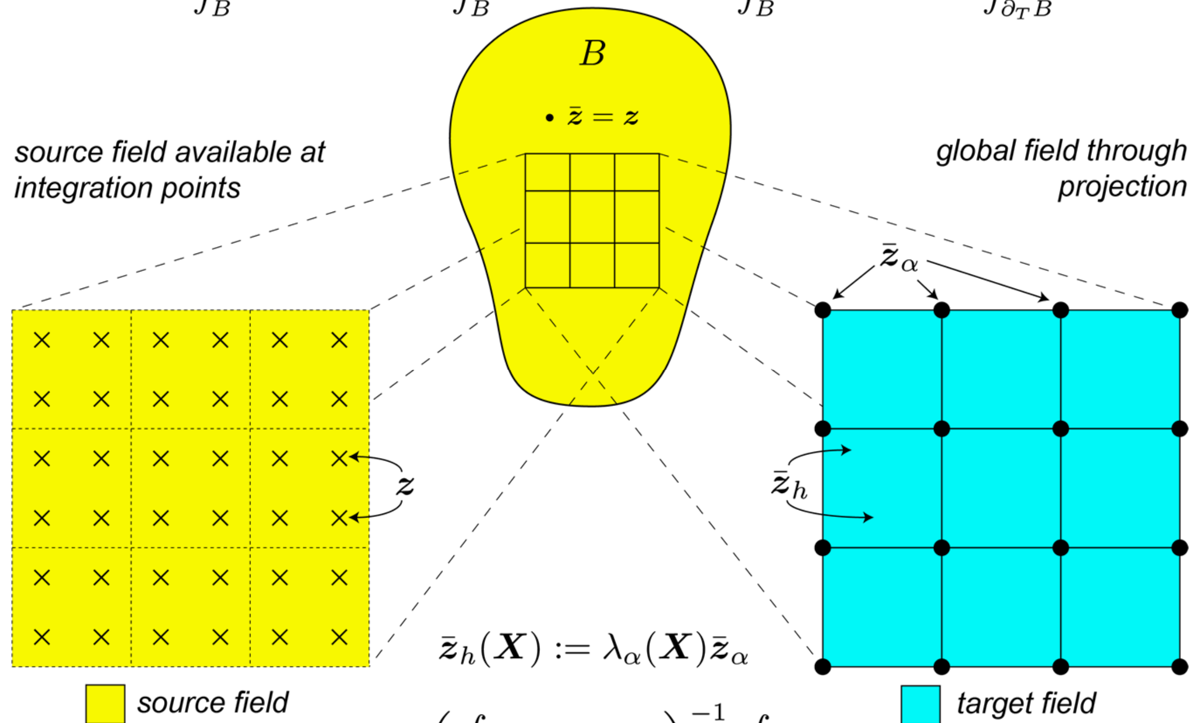

$$\bar{\boldsymbol{z}}_h(\boldsymbol{X}) := \lambda_\alpha(\boldsymbol{X})\bar{\boldsymbol{z}}_\alpha$$

$$\bar{\boldsymbol{z}}_h = \lambda_\alpha \left(\int_B \lambda_\alpha \lambda_\beta \boldsymbol{I}\, dV \right)^{-1} \int_B \lambda_\beta \boldsymbol{z}\, dV$$

- The variational principle naturally yields an optimal, L_2 projection
- The spaces of variables (Lie algrebra, Lie Group) are honored through log() and exp()
- Advocated by Mota, et. al., Computational Mechanics, 2013

  Past works: Ortiz and Quigley (1991), Radovitzky and Ortiz (1999), Rashid (2002), Jiao and Heath (2004)

We use tetrahedral elements

Motivated by prior work of Thoutireddy, et. al., IJNME (2002)

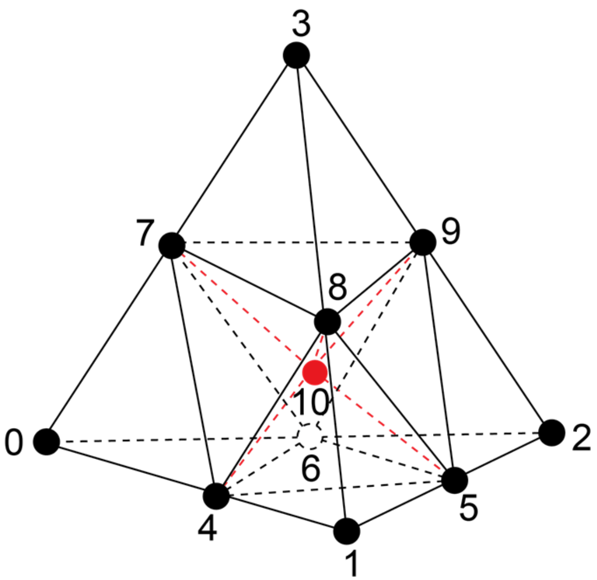

$$\bar{B}_{aJ}(\boldsymbol{X}) = \lambda_c(\boldsymbol{\xi})\left[\int_{\Omega_0} \lambda_c\lambda_b \, dV_0\right]^{-1} \int_{\Omega_0} \lambda_b N_{a,J} \, dV_0$$

$$\bar{B}_{aJ}(\boldsymbol{X}) = \lambda_c(\boldsymbol{\xi})\left[\int_{\Omega_\xi} \lambda_c\lambda_b \, dV_\xi\right]^{-1} \int_{\Omega_\xi} \lambda_b \frac{\partial N_a}{\partial \xi_k} \, dV_\xi \left(\frac{\partial \xi_k}{\partial X_J}\right)$$

$$\bar{B}_{aJ}(\boldsymbol{X}) = \bar{L}_{ak}(\boldsymbol{\xi})\xi_{k,J}$$

$$\bar{L}_{ak}(\boldsymbol{\xi}) = \lambda_c(\boldsymbol{\xi}){M_{cb}}^{-1} \int_{\Omega_\xi} \lambda_b \frac{\partial N_a}{\partial \xi_k} \, dV_\xi$$

$$\bar{L}_{ak}(\boldsymbol{\xi}) = \lambda_c(\boldsymbol{\xi})M_{cb}^{-1} \sum_{S=0}^{11} \frac{\partial N_a}{\partial \xi_k} \int_{E_S} \lambda_b \, dV_\xi$$

IDEA: Chain rule!

$$\frac{\partial N_a}{\partial X_J} = \frac{\partial N_a}{\partial \xi_K}\left(\frac{\partial X_J}{\partial \xi_K}\right)^{-1}$$

$$\bar{L}_{ak}(\boldsymbol{\xi}) = \begin{pmatrix}
\frac{1}{8}(-17+20\xi_1+20\xi_2+20\xi_3) & \frac{1}{8}(-17+20\xi_1+20\xi_2+20\xi_3) & \frac{1}{8}(-17+20\xi_1+20\xi_2+20\xi_3) \\
-\frac{3}{8}+\frac{5\xi_1}{2} & 0 & 0 \\
0 & -\frac{3}{8}+\frac{5\xi_2}{2} & 0 \\
0 & 0 & -\frac{3}{8}+\frac{5\xi_3}{2} \\
-\frac{35}{12}(-1+2\xi_1+\xi_2+\xi_3) & \frac{1}{12}(-4-35\xi_1+5\xi_2+10\xi_3) & \frac{1}{12}(-4-35\xi_1+10\xi_2+5\xi_3) \\
\frac{1}{12}(-1+5\xi_1+40\xi_2-5\xi_3) & \frac{1}{12}(-1+40\xi_1+5\xi_2-5\xi_3) & -\frac{5}{12}(-1+\xi_1+\xi_2+2\xi_3) \\
\frac{1}{12}(-4+5\xi_1-35\xi_2+10\xi_3) & -\frac{35}{12}(-1+\xi_1+2\xi_2+\xi_3) & \frac{1}{12}(-4+10\xi_1-35\xi_2+5\xi_3) \\
\frac{1}{12}(-4+5\xi_1+10\xi_2-35\xi_3) & \frac{1}{12}(-4+10\xi_1+5\xi_2-35\xi_3) & -\frac{35}{12}(-1+\xi_1+\xi_2+2\xi_3) \\
\frac{1}{12}(-1+5\xi_1-5\xi_2+40\xi_3) & -\frac{5}{12}(-1+\xi_1+2\xi_2+\xi_3) & \frac{1}{12}(-1+40\xi_1-5\xi_2+5\xi_3) \\
-\frac{5}{12}(-1+2\xi_1+\xi_2+\xi_3) & \frac{1}{12}(-1-5\xi_1+5\xi_2+40\xi_3) & \frac{1}{12}(-1-5\xi_1+40\xi_2+5\xi_3)
\end{pmatrix}$$

$$\bar{B}_{aJ}(\boldsymbol{X}) = \bar{L}_{ak}(\boldsymbol{\xi})\left(X_{Jb}\bar{L}_{bk}(\boldsymbol{\xi})\right)^{-1}$$

This is exact. Evaluate for your flavor of cubature.

We adopt a new reference configuration

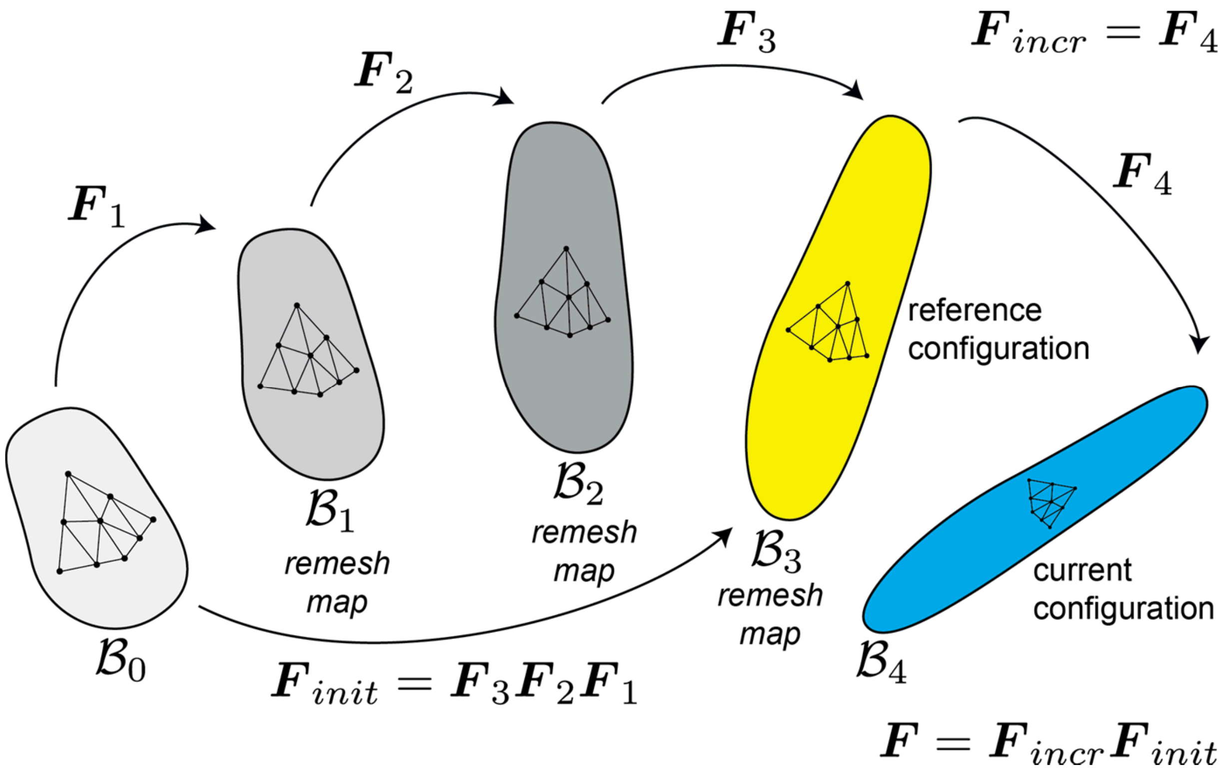

- Prior work on hexahedral elements maintained the reference configuration
- Elements degrade in the reference configuration - T-L element integrate in reference
- We now adopt a new reference configuration and map $\mathbf{F}_{init}$ (which lives in a Lie Group)

We accommodate local remeshing

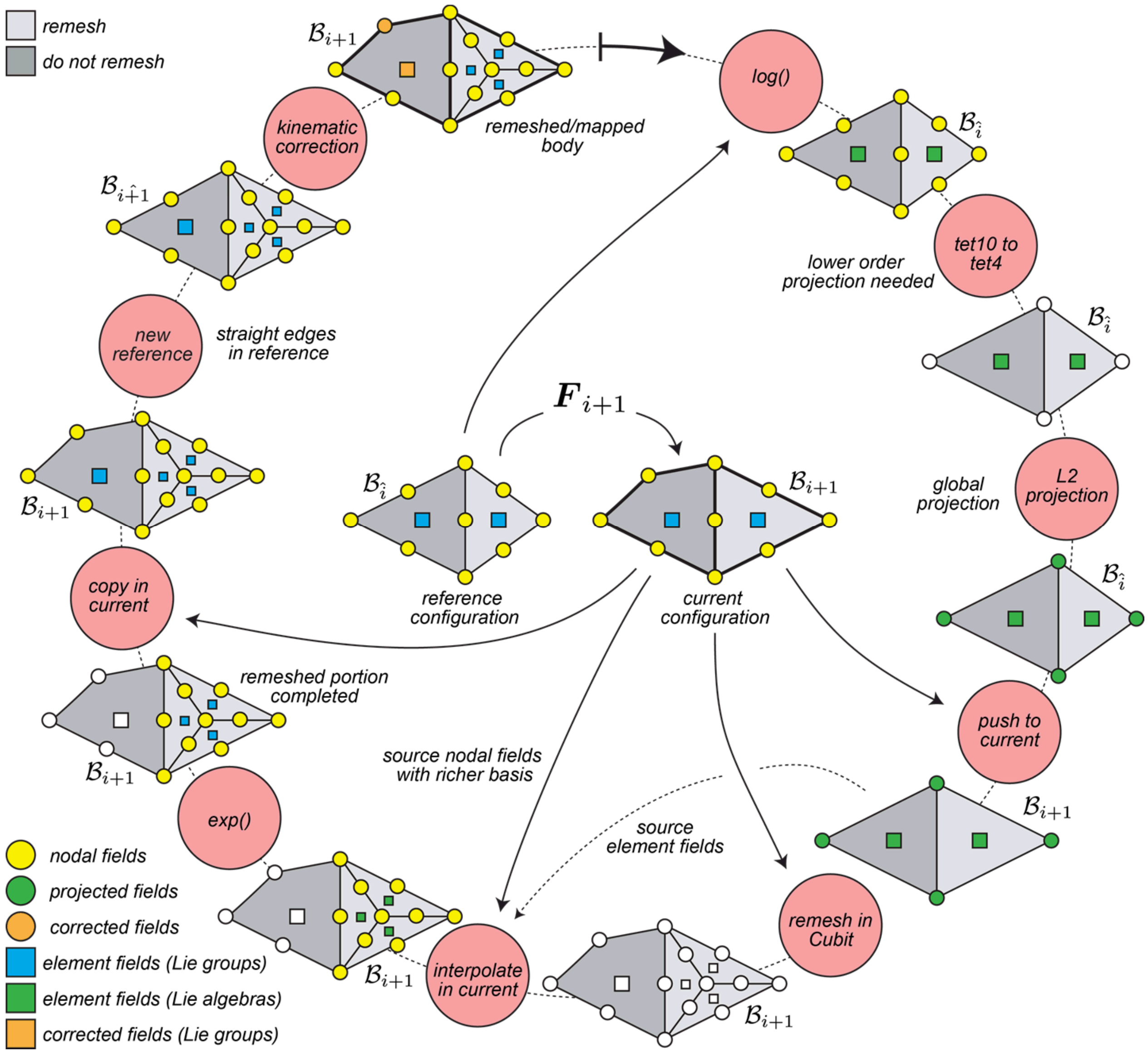

This methodology is completely general to element type and constitutive model.

Efforts to simulate ductile failure at the microstuctural level are burdened with an explicit representation of void evolution. Remeshing needed.

Move over bar. Cubes can neck too.

initial configuration | *117 maps* | *178 maps* | *235 maps*

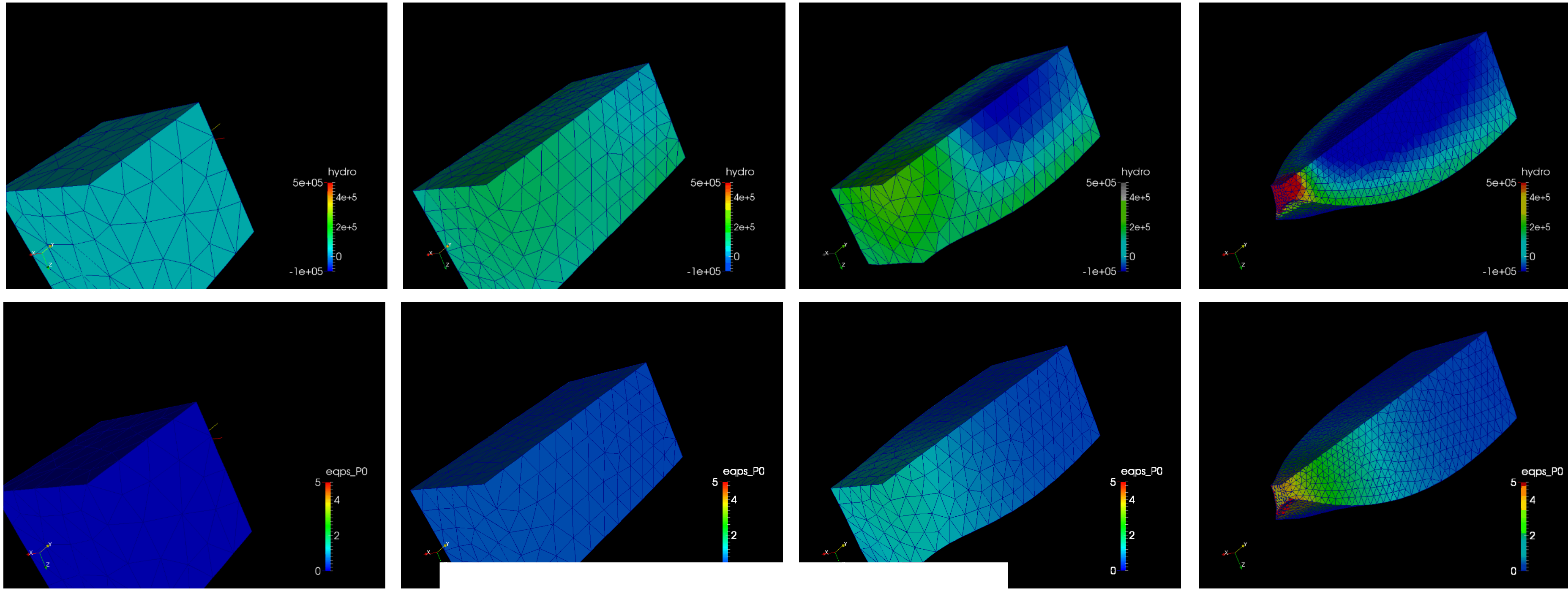

Unit cube w/symmetry. Pull "top" and keep 5 elements at "waist"

235 remesh/map steps

Plastic strains > 500%
Pressure is smooth

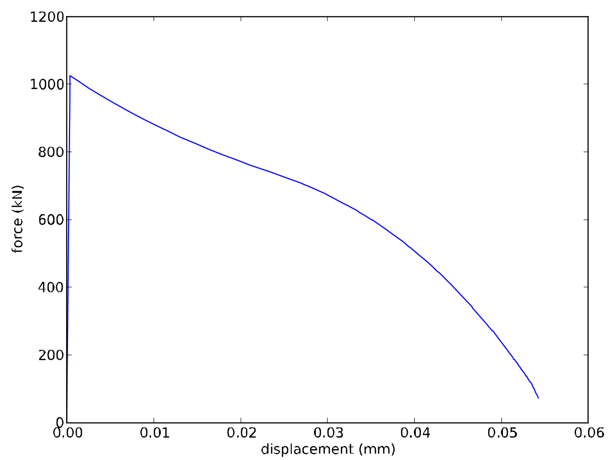

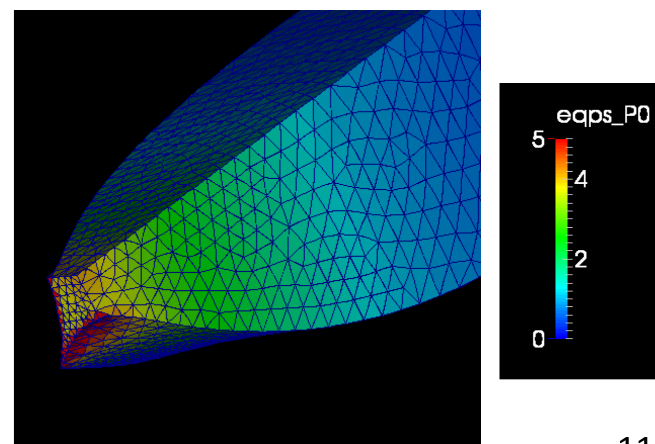

Every frame is another circle of remeshing and mapping

Sandia National Laboratories

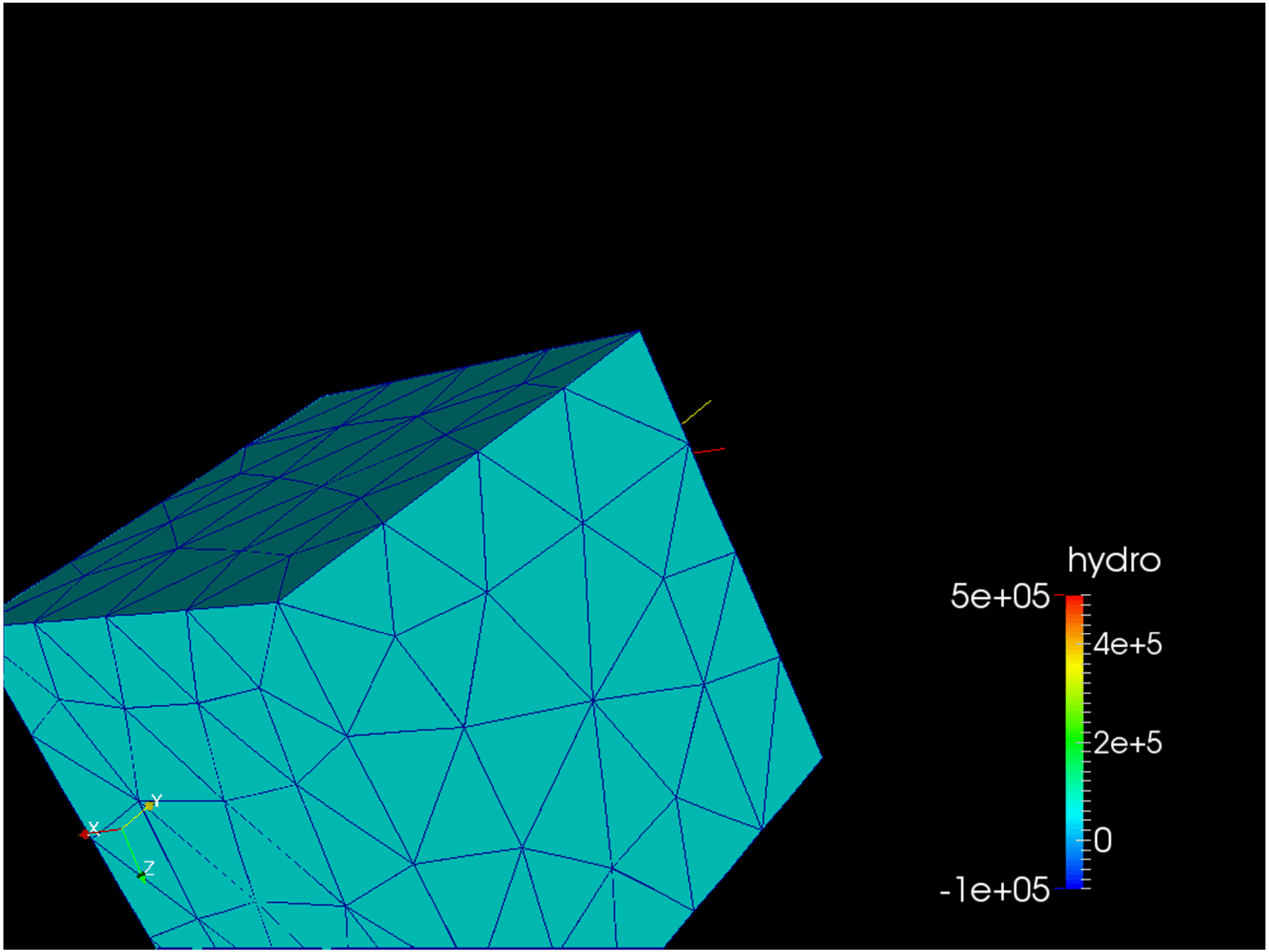

Can we now model the loss of load-bearing capacity? Yes

We only remesh local element blocks (blue)

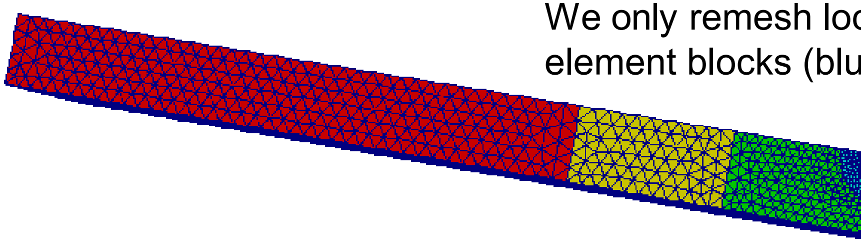

Composite-Tet10
Elements: 110,944
Nodes: 163,444
Yield stress: 196 MPa
Hardening: 2360 MPa
Recovery: 1.3

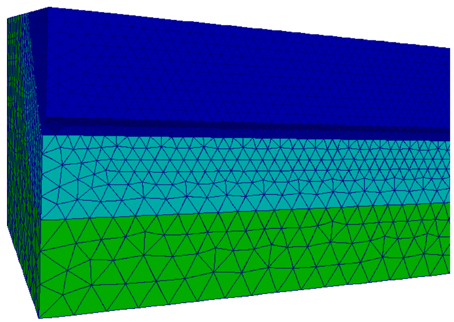

$$\sigma_y = Y + \kappa \qquad \dot{\kappa} = [H - R\kappa]\,\dot{\epsilon}_p$$

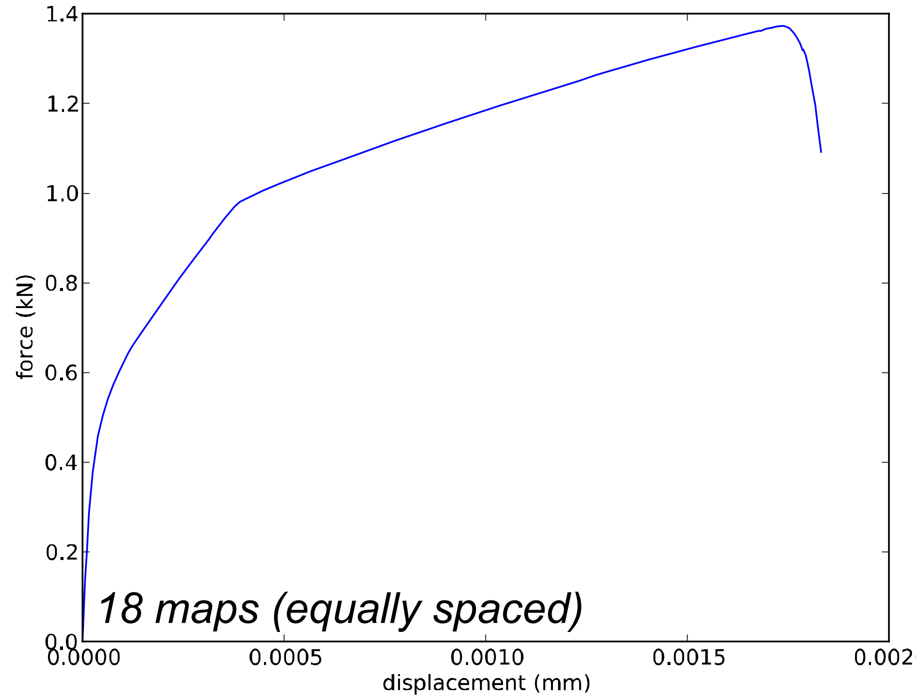

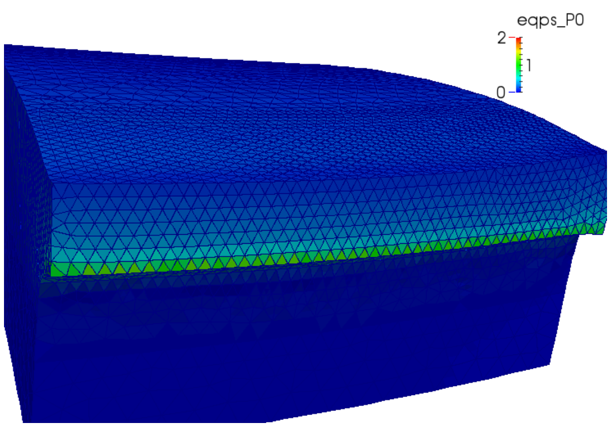

12th map

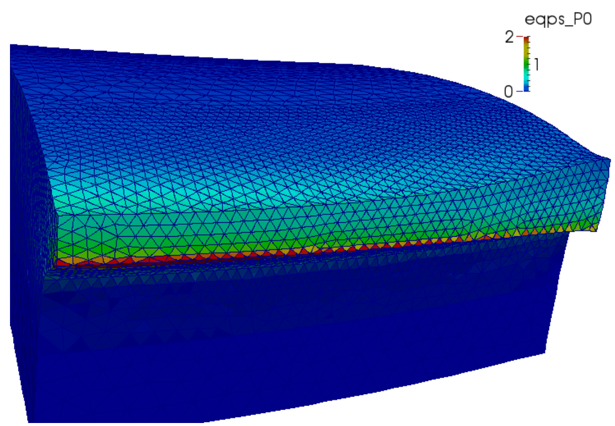

17th map

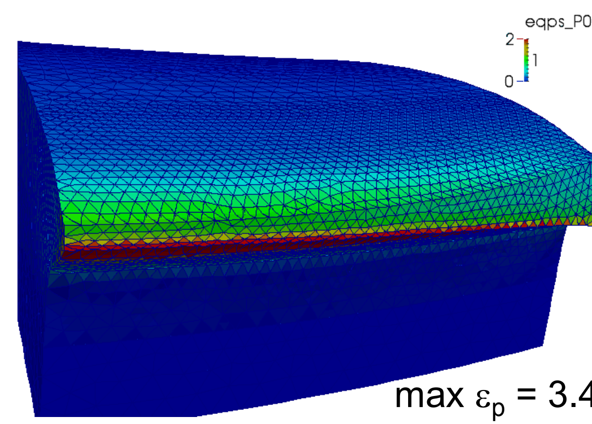

18th map

Additional interior and exterior views of necking

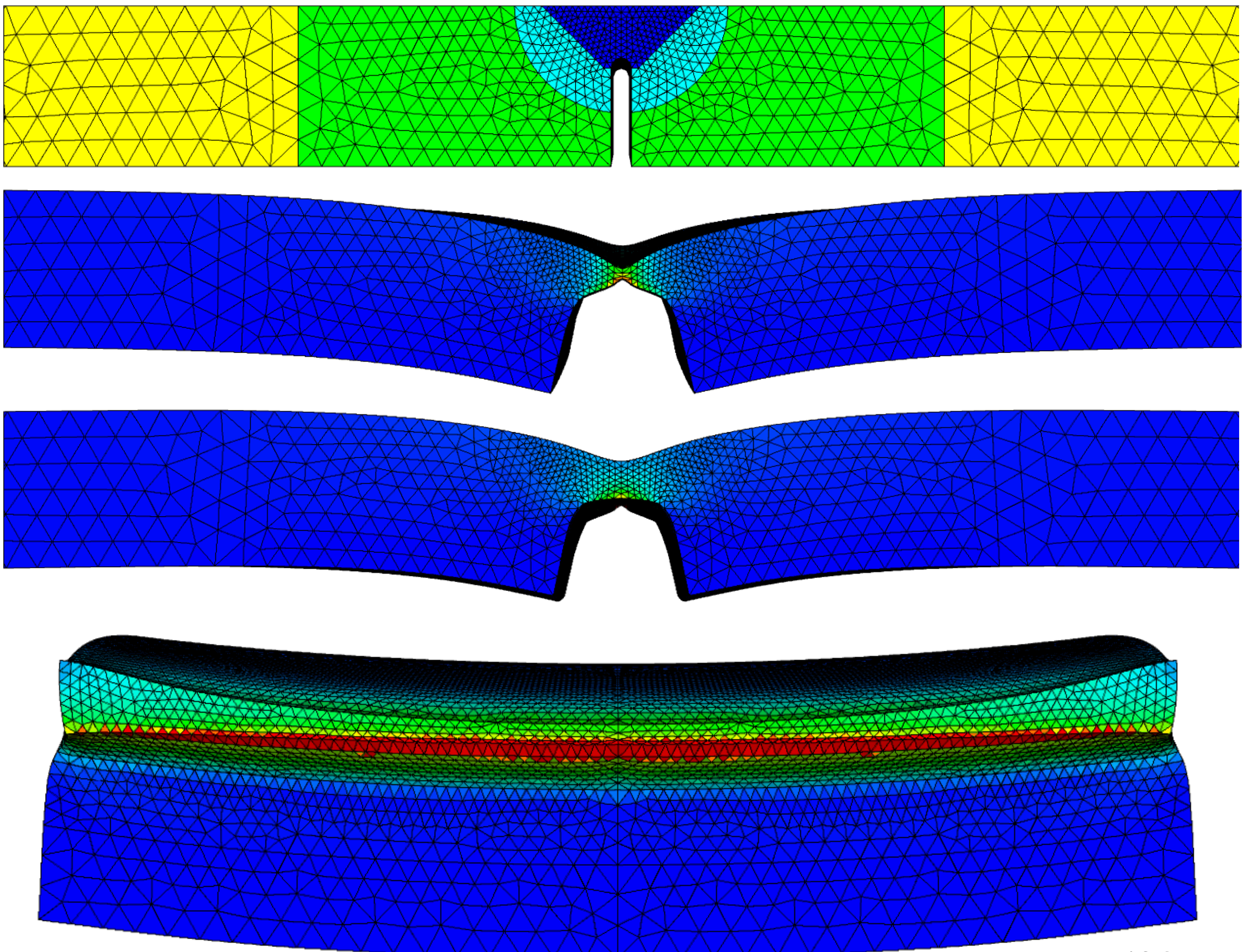

undeformed mesh with notch

necking at mid-plane

necking at surface

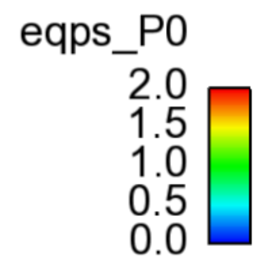

max ε_p = 3.4

18th map

Progress in modeling the evolution of pore structures

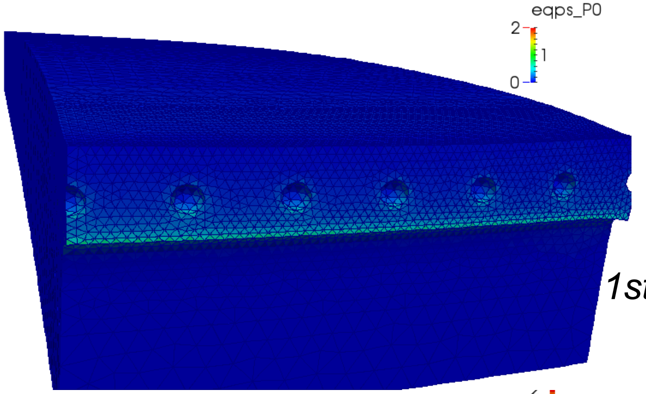

1st map

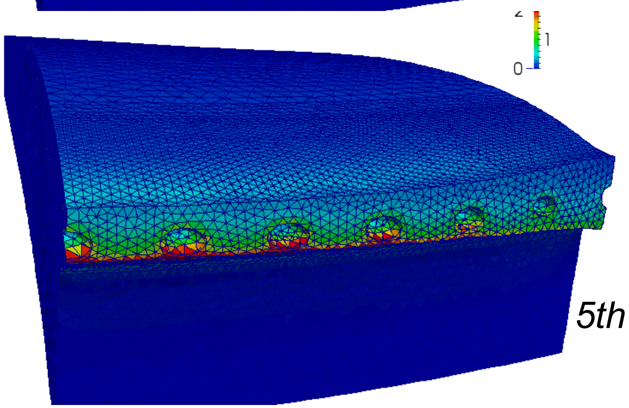

5th map

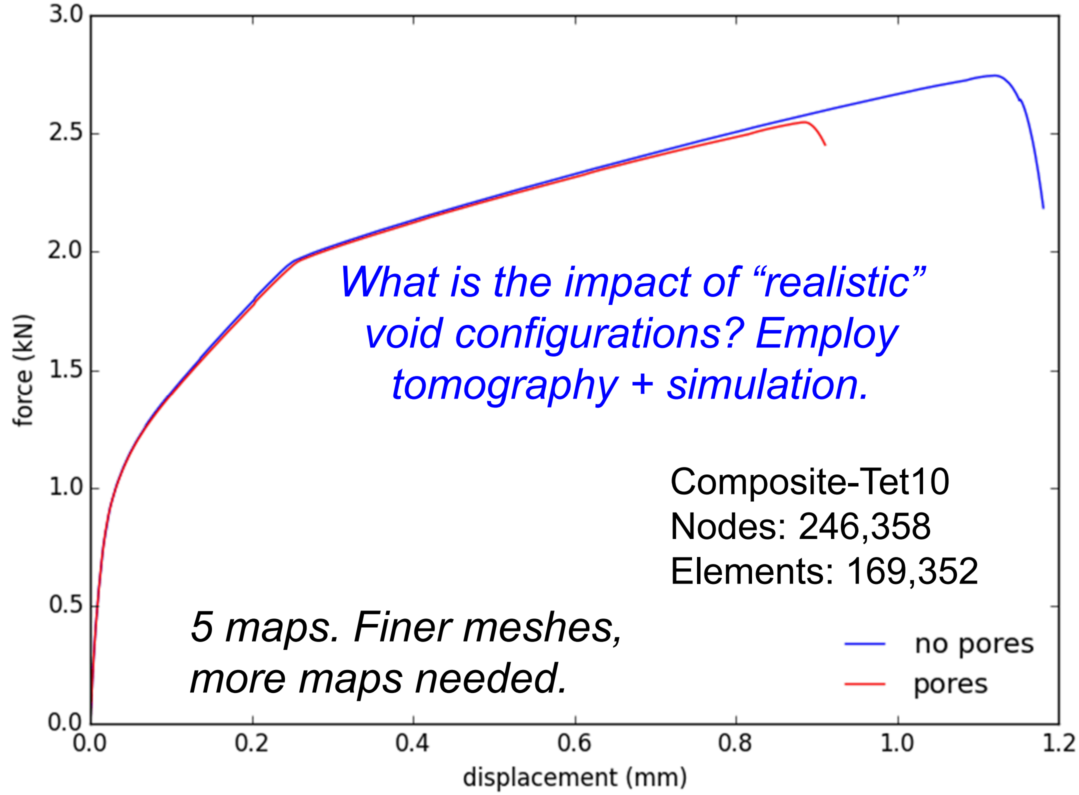

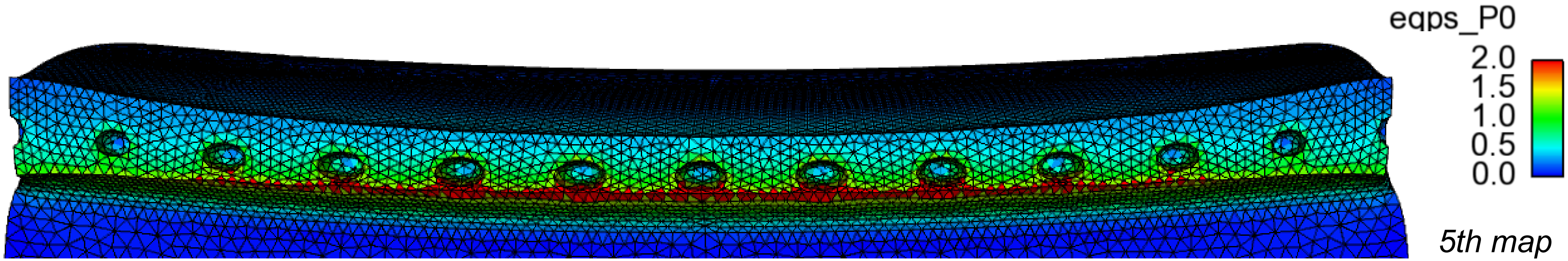

5th map

Additional interior and exterior views of necking w/pores

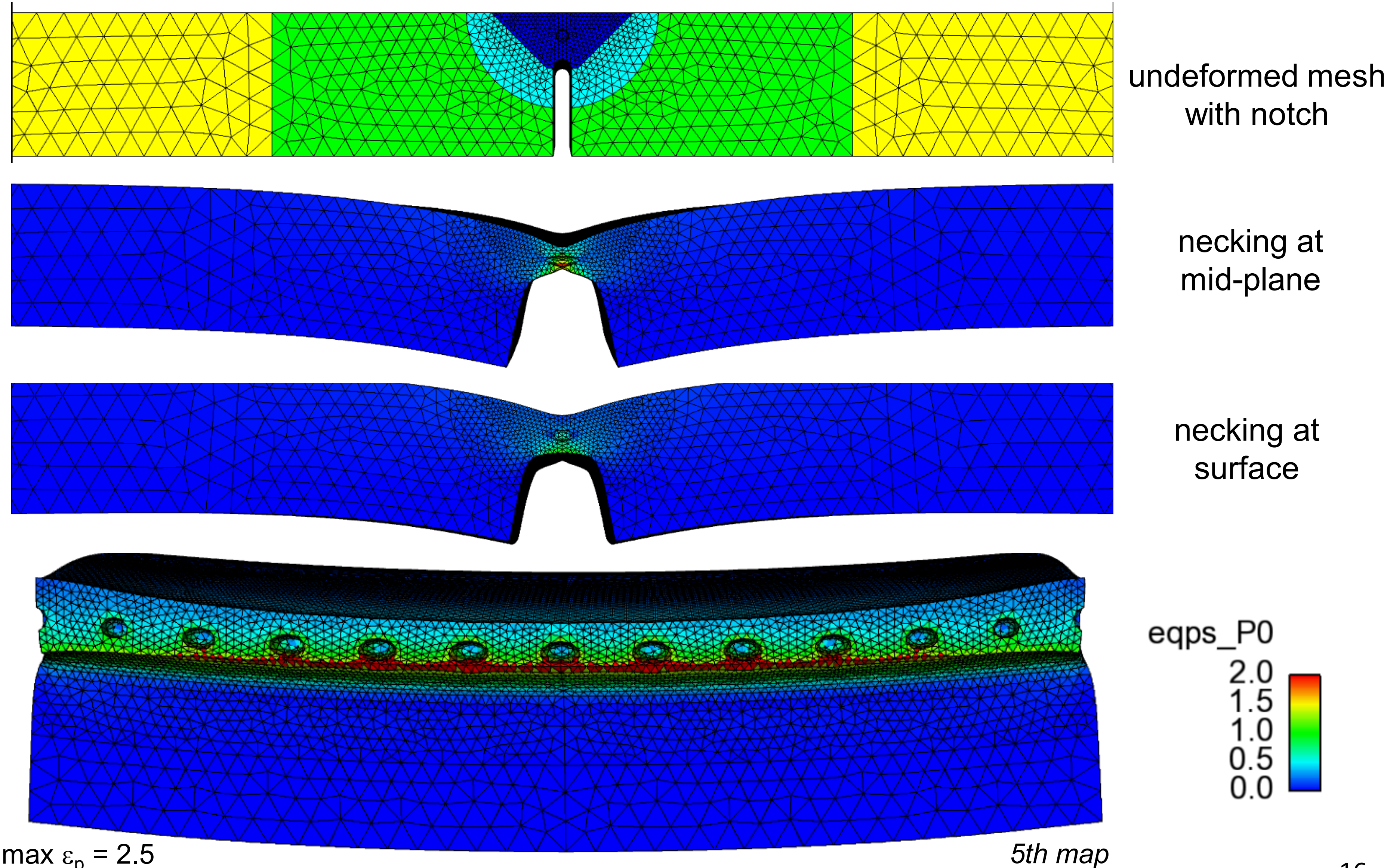

Increasing the number of mappings

Animation illustrating the deformation process with 31 maps

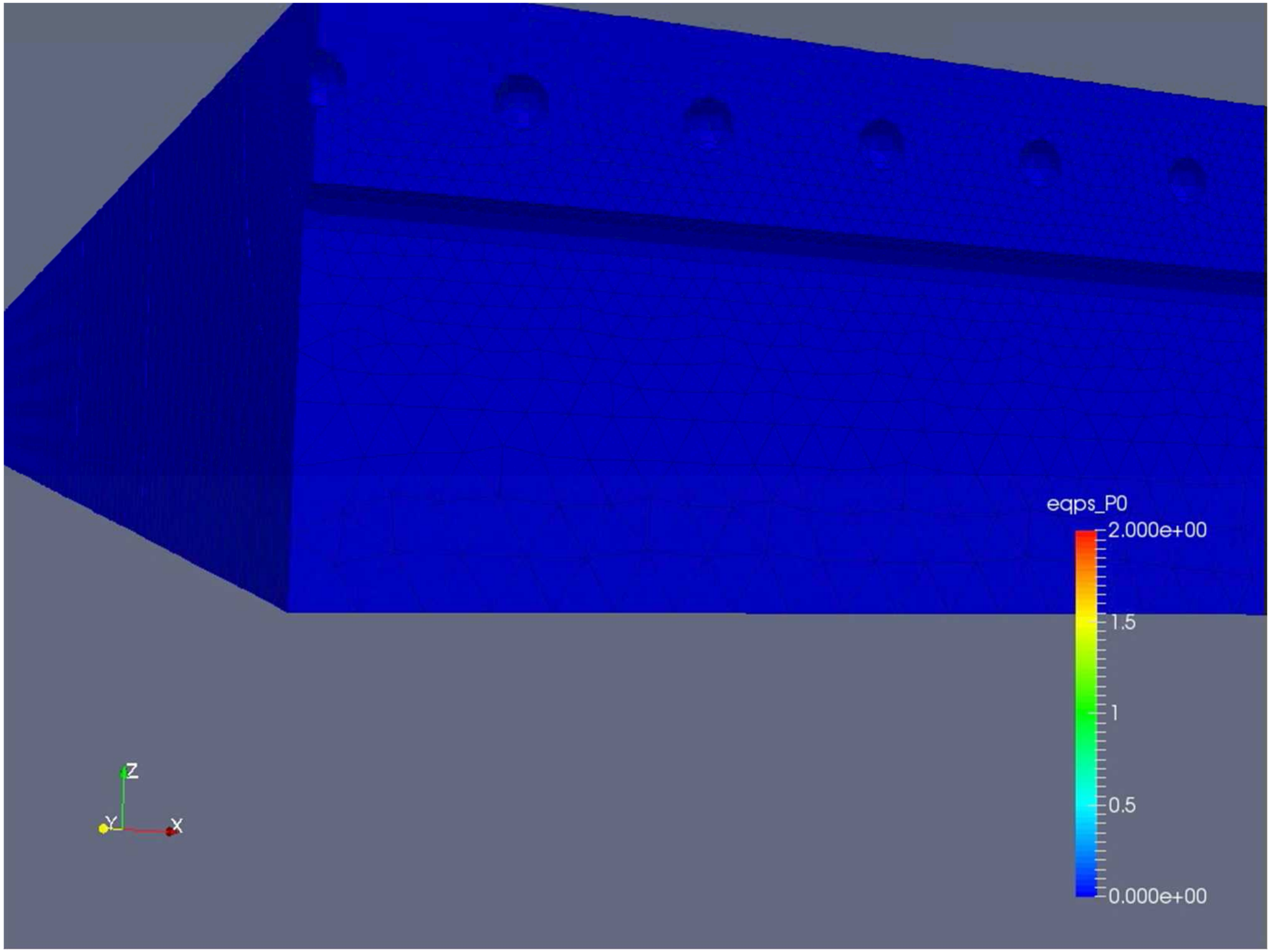

Conclusions and Path forward

- *mapLL* ensures a sound theoretical basis
- Tetrahedral elements permit discretization
- Composite-tetrahedral elements resolves ISVs
- New reference configuration enables solution
- We are able to predict the load-bearing capacity
- General methodology for modeling localization

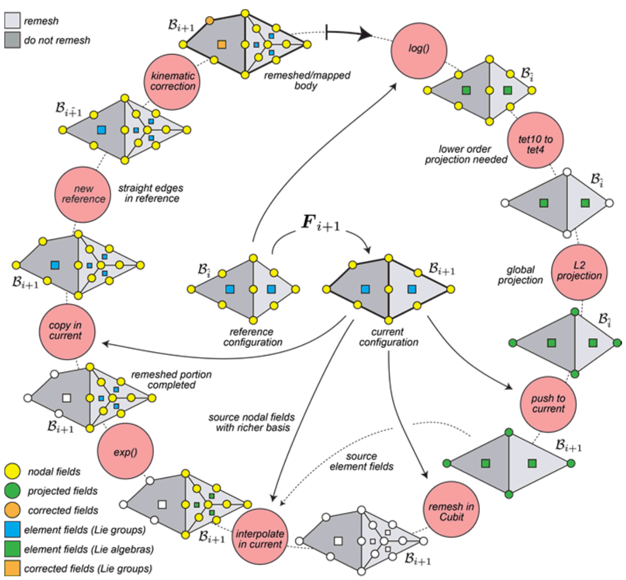

- Re-examine convergence
  - Mesh refinement
  - # maps / # intervals
- Solidify remeshing/mapping
- Model idealized void configurations
- Connect void structure to weld performance

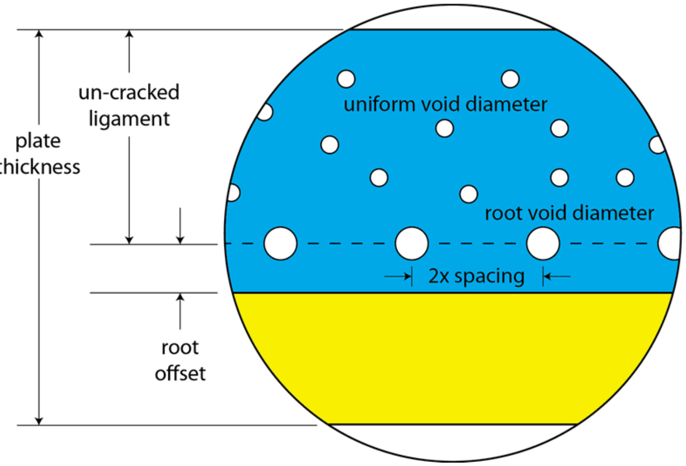

Numerous remaps exhibits minimal “diffusion” of ISVs

Equivalent plastic strain in fine mesh at one integration point per element at t = 0.25

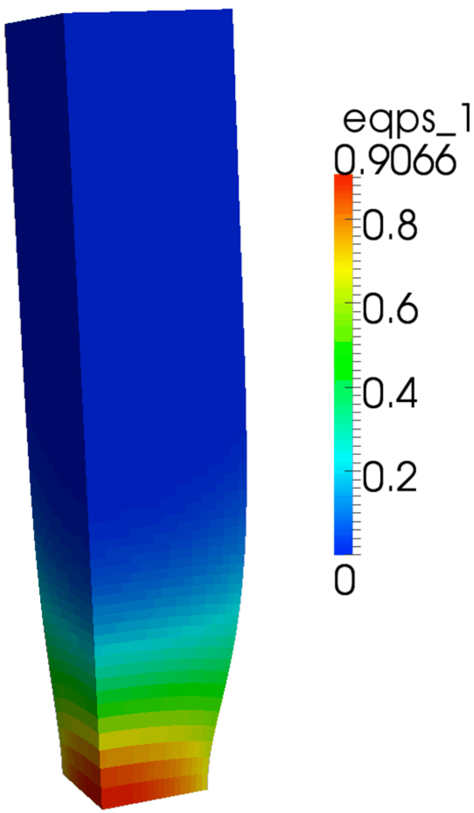

no mapping

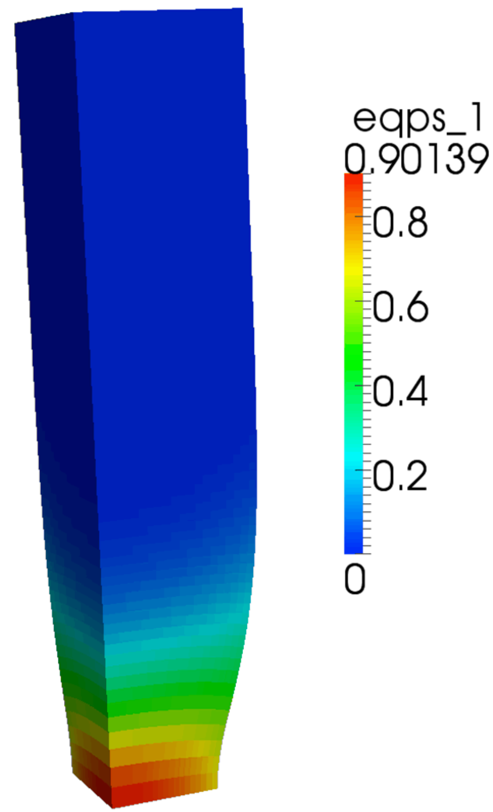

map 100 times between t = 0 and t=0.25

Repeated mapping convergent in global and field quantities

Maximum plastic strain converges

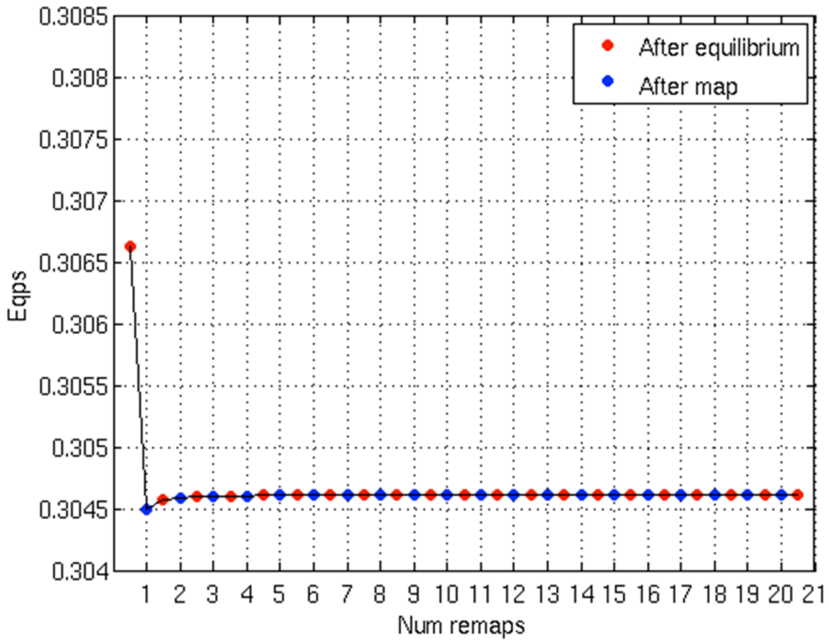

Initial residual decreasing with additional mappings

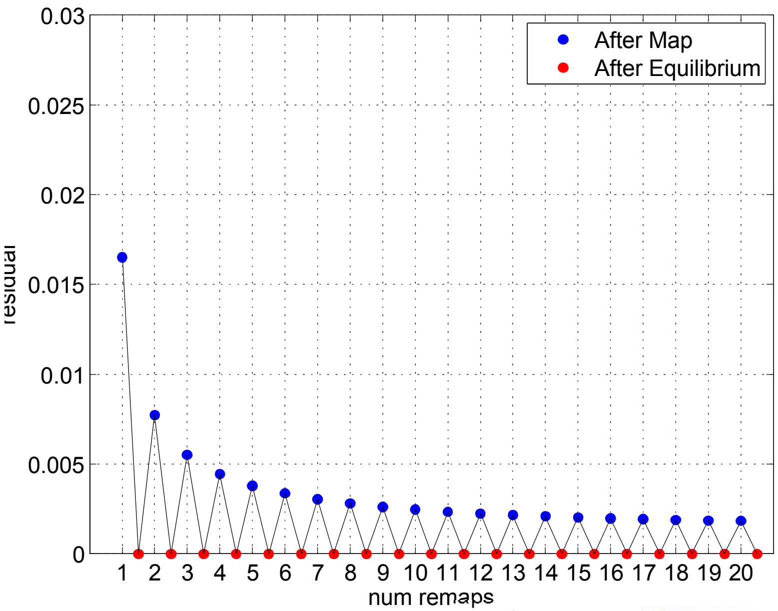

The system comes back into equilibrium rapidly, i.e. only a few iterations.

The residual after mapping may be an indication of the discretization error. Investigation into different levels of refinement are needed.

Difference in magnitude of residual

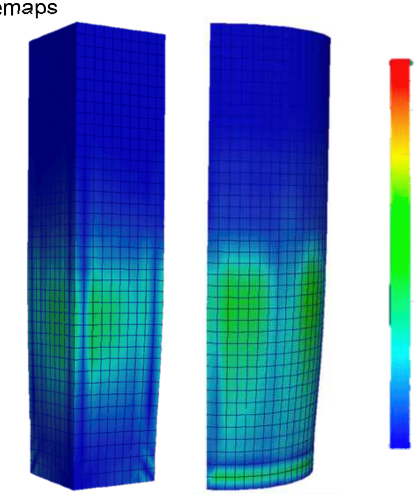

Include remeshing in automated procedure

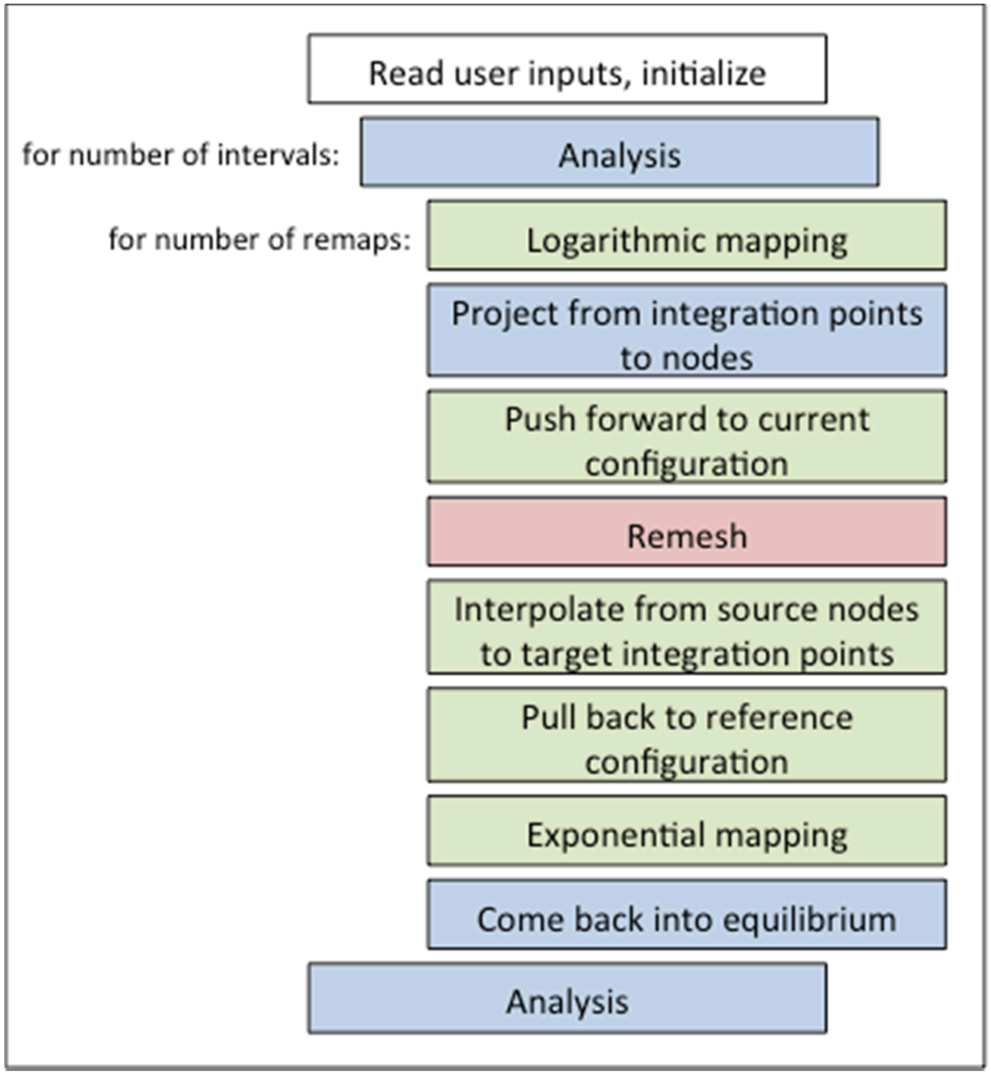

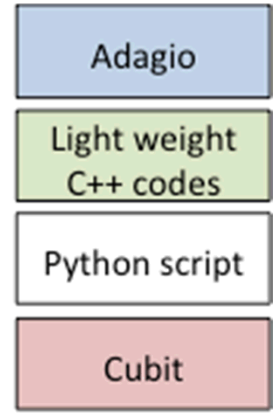

NOTE: This scheme keeps the reference configuration

Converged meshes not sensitive to remeshing/mapping

25x refers to 25 mapping and remeshing procedures

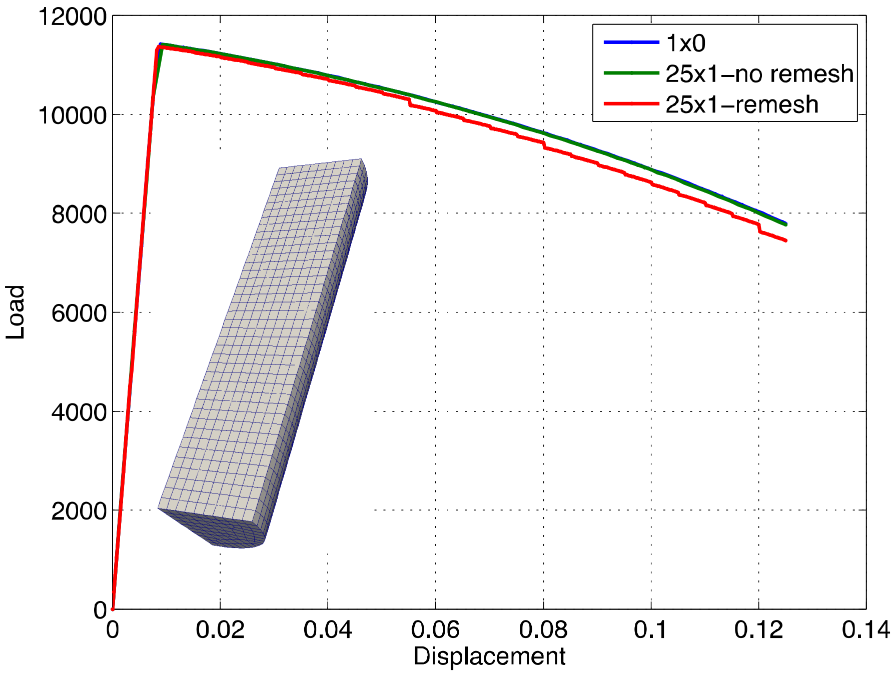

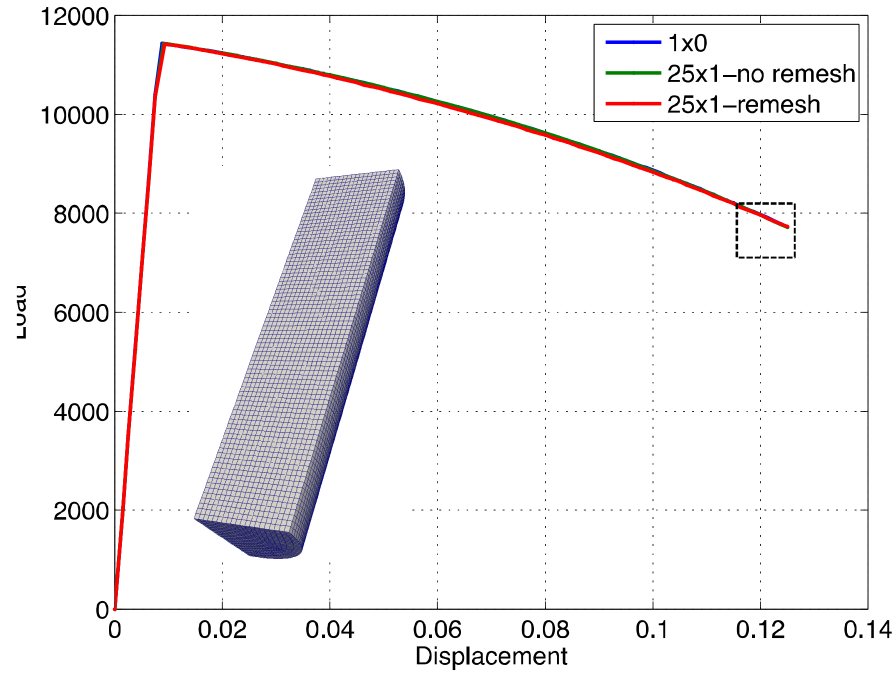

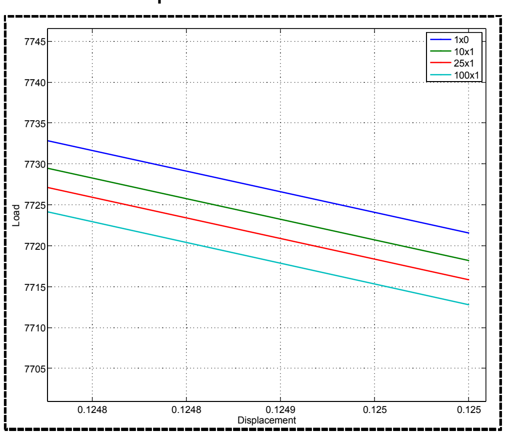

NOTE: Discretizations with resolved (converged) fields of internal state variables are less sensitive to the remeshing/mapping procedures.

Are we any closer to our goal? Yes and no.

Hexes look great, but….

- Meshing of arbitrary geometries requires tetrahedral elements
- Composite tet10 formulation not robust for isochoric motions
- Consistent projection for piecewise linear tet10 is flawed
- Total-Lagrange elements will require a new reference configuration

We did not hesitate to address these fundamental issues (no shortcuts)

- We will use tetrahedral elements. Period.
- Derive an analytical gradient operator for composite tet10
- Volume averaging J yields smooth pressure fields under isochoric motions
- Employ linear projection (tet4) for higher-order tetrahedral elements
- Establish a new reference configurations for T-L elements through $\boldsymbol{F}_{init}$